Ingeniería Investigación y Tecnología
volumen XXV (número 2), abril-junio 2024 1-12
ISSN 2594-0732 FI-UNAM artículo arbitrado
Información del artículo: Recibido: 21 de junio de 2023, aceptado: 11 de marzo de 2024

https://doi.org/10.22201/fi.25940732e.2024.25.2.015

Ingeniería
Investigación y
Tecnología

Efficient coil design for transcranial magnetic stimulation using computational tools

Diseño eficiente de bobinas para estimulación magnética transcraneal utilizando herramientas computacionales

Ramirez-Galindo Angel D.
Universidad Autónoma Metropolitana (UAM), Unidad Azcapotzalco
Departamento de Energía
E-mail: angeldram698@gmail.com
https://orcid.org/0000-0001-7922-4581

Olivares-Galvan Juan Carlos
Universidad Autónoma Metropolitana (UAM), Unidad Azcapotzalco
Departamento de Energía
E-mail: jolivares@azc.uam.mx (corresponding author)
https://orcid.org/0000-0002-1935-2669

Corona-Sánchez Manuel A.
Universidad Autónoma de la Ciudad de México
E-mail: manuel.corona@uacm.edu.mx
https://orcid.org/0000-0002-0530-6493

Escarela-Perez Rafael
Universidad Autónoma Metropolitana (UAM), Unidad Azcapotzalco
Departamento de Energía
E-mail: epr@azc.uam.mx
https://orcid.org/0000-0001-7415-3059

Melgoza-Vazquez Enrique
Instituto Tecnológico de Morelia, Michoacán
Tecnológico Nacional de México
Programa de Graduados e Investigación en Ingeniería Eléctrica
E-mail: emv@ieee.org
https://orcid.org/0000-0002-1809-8240

Gonzalez-Montañez Felipe de Jesús
Universidad Autónoma Metropolitana (UAM), Unidad Azcapotzalco
Departamento de Energía
E-mail: fjgm@azc.uam.mx
https://orcid.org/0000-0002-7113-1708

Abstract

In the last two decades, Transcranial Magnetic Stimulation (TMS) has been used in research protocols and clinical treatment of neurological disorders. In this work, we analyze the heating of a transcranial magnetic stimulation equipment, with the aim of reducing it using a novel design of stimulation coils. The operation of the equipment is limited by the overheating of the stimulation coils, such that the continuous use of the equipment during the therapy is impossible, and the device´s life time is affected. The first stage of the analysis consists of studying the response of the electrical excitation circuit through simulations, considering the use of concentric inductors to divide the magnitude of the current. This is complemented by multiphysical analysis with coupling between the magnetic field and heat transfer of two different coil geometries, showing the spatial distribution of the generated magnetic field and temperature rise in the space surrounding the stimulation coil. The main contribution of this research is the design of a stimulation coil using the finite element method, reducing the device´s operating temperature considering a practical coil geometry.
Keywords: Coils, electrical circuit, finite element method, induced electric field, Transcranial Magnetic Stimulation.

Resumen

En las últimas dos décadas, la Estimulación Magnética Transcraneal (TMS) se ha utilizado en protocolos de investigación y tratamiento clínico de trastornos neurológicos. En este trabajo se analiza el calentamiento de un equipo de estimulación magnética transcraneal, con el objetivo de reducirlo mediante un novedoso diseño de bobinas de estimulación. El funcionamiento del equipo está limitado por el sobrecalentamiento de las bobinas de estimulación, de manera que es imposible el uso continuo del equipo durante la terapia, y la vida útil del dispositivo se ve afectada. La primera etapa del análisis consiste en estudiar la respuesta del circuito de excitación eléctrica a través de simulaciones, considerando el uso de inductores concéntricos para dividir la magnitud de la corriente. Esto se complementa con un análisis multifísico con acoplamiento entre el campo magnético y la transferencia de calor de dos geometrías de bobina diferentes, que muestra la distribución espacial del campo magnético generado y el aumento de temperatura en el espacio que rodea la bobina de estimulación. El principal aporte de esta investigación es el diseño de una bobina de estimulación utilizando el método de elementos finitos, reduciendo la temperatura de operación del dispositivo considerando una geometría práctica de bobina.
Descriptores: Bobinas, circuito eléctrico, método de elemento finito, campo eléctrico inducido, Estimulación Magnética Transcraneal.

https://doi.org/10.22201/fi.25940732e.2024.25.2.015

Introduction

Neuropsychiatric conditions are increasingly common, both in young and older people. The applied medical treatments consist mainly of psychotherapeutic sessions and controlled medications; however, they are proven ineffective in some cases due to different factors such as pharmacological resistance, high cost of treatments, or unwillingness of patients to use medications. Along with the evolution of the existing treatment methods, alternative therapies have emerged to reduce these conditions occurrence or control symptoms. Transcranial Magnetic Stimulation (TMS) is one of these emerging therapies; its efficacy has been proven in different clinical protocols for psychological conditions, as well as in the research area where the effects of stimulation at cellular and molecular levels have been observed. TMS consists of a non-invasive stimulation of brain tissue by means of electric fields induced with a magnetic field generator that produces pulses of high intensity (about 1 T, focused on human use in clinical treatments) (Maertens, 2006). There are applications where low-intensity fields are generated (between 1 and 3 mT); however, these are focused on the research area where small mammals or cell cultures are stimulated (Túnez *et al.,* 2006). The aim of TMS is to increase or depress the activity of neurons in order to strengthen or weaken neuronal synapses. These effects are produced mainly in superficial structures such as the cerebral cortex, which controls different brain and spinal nuclei (Oliveiro *et al.,* 2011; Vlachos *et al.,* 2012). The TMS of the cerebral cortex has demonstrated the inhibition and facilitation of functions of certain neuronal structures, including those involved in perception, motor execution, or higher-level cognitive processes. Repetitive transcranial stimulation is a promising tool to explore the inhibitory and excitatory properties of various cortical brain areas in normal subjects, as well as its connectivity with distant areas of the nervous system (Maertens, 2006). Oliviero *et al.* (2011) report reduced motor cortex function for a few minutes after stimulation application due to reduced neuronal excitability in the area. Favorable results have been presented in the study of functional plasticity, according to Vlachos *et al.* (2012) in cell cultures of mouse hippocampal slices. Promising treatments have been reported for psychological disorders such as depression in drug-resistant patients (Zanardi *et al.,* 2006), analyzing cognitive effects in late-life depression (Kaster *et al.,* 2018), patients' resistance to any treatment for depression (Van den Noort *et al.,* 2018), anxiety and stress, among others. An essential factor in the stimulation systems is the geometry of the coils; the most commonly used geometry is the eight-shaped coil (Hardwick *et al.,* 2014). Opitz *et al.* (2011) characterized the electric field induced in the brain by calculating EMF (electromotive force) based on a high-resolution model of the volume of a head. A problem reported in some research articles is the study of hyperthermia produced by the use of high-energy electromagnetic fields; so far, these effects of increased temperature are attributed to the field; however, heating the stimulation equipment can have a considerable effect. See table A for a comparison of the existing TMS systems with the system proposed in this investigation.

Considering these limitations in current stimulation equipment, we present a novel design for the TMS coil with the aim of reducing the power dissipated as heat by the stimulation coil. The goal is to reduce the downtime of the TMS equipment required to cool it, since commercial equipment is usually cooled down using airflow systems for around 5 minutes, between sessions ("Medical Expo", n.d.). During these 5 minutes the TMS equipment is not used and the patient must wait to continue with the treatment. TMS equipment consists of an RLC circuit including power electronics elements (MOSFET, diodes, etc.), whose operation shapes the waveform to energize the stimulation coil and the current pulses necessary to produce a physiological effect in safe operating ranges, avoiding the resonance condition of the RLC circuit. In the present work we are interested in the operating conditions that eliminate the resonance phenomenon. In this research, we analyze the TMS simple solenoid coil and Figure-8 coil, typically used in clinical applications, using the finite element method. Considering the excitation current provided by the TMS circuit we can obtain the magnetic flux density and the maximum operating temperature. The results found here indicate that the stimulation coil's maximum operating temperature is reduced by 20 °C.

Transcranial Magnetic Stimulation

TMS is a non-invasive brain stimulation technique that involves the induction of an electric field in brain tissue to modulate the activity of the nerves and the cortex. The effect achieved by this technique is to induce a change in the neuronal membrane potential. The cell membrane of neurons can be modeled by an equivalent electrical circuit, which describes the electric potential between the internal and external environment of the cell (Davey & Epstein, 2000). Physically, the stimulation generates a movement of charges through the neuronal membrane. When the accumulation of charges reaches a limit, the potential difference can no longer be maintained, and a depolarization is produced. The energy required to reach this stimulation threshold is descri-

bed as a function of the magnetic flux density B and time (Ori *et al.*, 2018).

The time to return to a resting state is known as the refractory period; this period must be respected as much as possible to avoid fatigue in the cells. However, the neuronal activation required to treat some neuropsychiatric conditions dictates that this refractory period be shorter than normal. The time constant that determines this is known as $\tau_{m,}$ and it is defined as the product of the resistance and capacitance of the equivalent circuit (Pastor, 2000).

A basic connection diagram illustrating the interface between the human brain and the transcranial magnetic stimulation system is available in Figure 1 (Epstein & Eric, 2008).

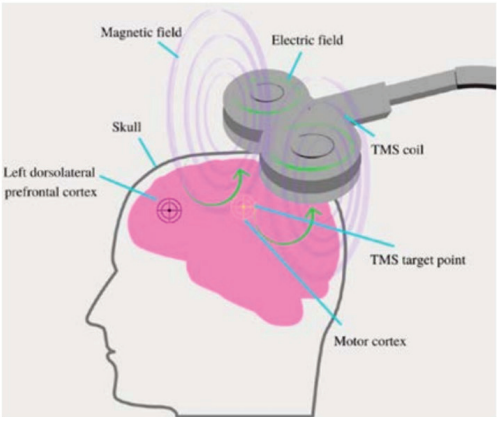

Figure 1. A basic connection diagram illustrating the interface between the human brain and the transcranial magnetic stimulation system

Excitation circuit of TMS

The electric circuit of a TMS system, shown in Figure 2, can be divided into three stages: rectification stage, switching stage, and RLC circuit charging and discharging stage (Selvaraj *et al.*, 2018; Roth *et al.*, 2007).

The circuit's first stage is associated with the power supply. In most design works, the electrical circuit is simplified considering a DC source; however, in a more complete analysis, an alternating current rectification stage is considered, possibly using a step-up transformer to get the proper voltage. The full wave rectification stage consists of a diode bridge and a capacitor as a filter. Both components must be able to withstand the voltage of the power source.

The second stage performs the switching and consists of a transistor. In this case, the effect of an N channel MOSFET is analyzed (positive drain-source voltage and positive gate-source voltage). This element works like a switch placing a voltage on the gate terminal to activate or deactivate the voltage between the drain-source terminals. The MOSFET is chosen as the switching element since the opening and closing control is done by voltage and not by current; unlike a BJT or IGBT, it stops thermal dispersion naturally, it has an internal diode to avoid the reverse flow of current and is highly recommended for use in switching power systems. The opening and closing voltages are controlled by an external system which must generate the pulses associated with the stimulation protocols.

The third stage is the charge and discharge of the LC circuit. The geometry of the stimulation coil determines the resistance and inductance values of the RLC circuit. Therefore, the design of this stage will depend on the induced biological response. Also, the parameters of the elements in this stage must fall within permissible limits, namely 10–25 μH and 50 – 1500 μF for the inductor and capacitor, respectively.

The value of the inductor will also depend on the geometry used, so it can be considered as a parameter determined by the information provided by the manufacturers.

An important parameter is the resonance frequency; this phenomenon in a series RLC circuit causes the inductive and capacitive effects to cancel out, turning the circuit into a purely resistive one with a maximum current flow (Figure 2).

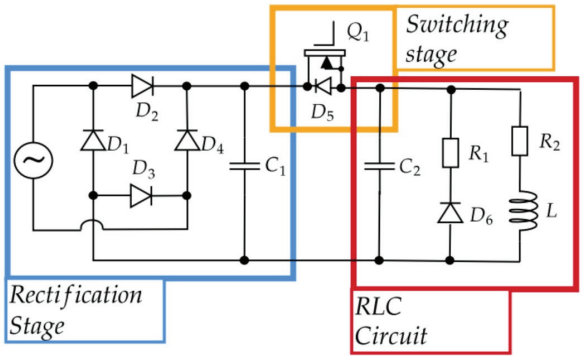

Figure 2. TMS Excitation Circuit Stages

For the performed simulation, a source of 2000 V and 60 Hz are proposed to be consistent with the calculations made. Subsequently, the rectified value is about 1700 V with 3000 A. A pulse train is used for the switching stage with a continuous frequency of 2 kHz and an amplitude of 5 V connected to the gate terminal of the block associated with the MOSFET. Finally, we consider the shape and amplitude of the voltage across the capacitor (v_o) and the current in the inductor (i_L). The simulation results are shown in Figure 3. The line voltage is shown in green, the rectified voltage in orange, the square pul-

https://doi.org/10.22201/fi.25940732e.2024.25.2.015

ses of the switching stage in purple, the shape of the charge and discharge signal of the capacitor in blue, and finally, the current that flows through the inductor in red.

When the circuit oscillates at the resonance frequency, the elements may be destroyed (Floyd *et al.*, 2019). The determination of the resonance frequency is based on the time that an electromagnetic pulse must be applied to the brain tissue to produce a physiological effect, that is $\tau\_m = 152 \pm 26$ μs for stimulating the neurons in the cerebral cortex (Ori *et al.*, 2018). Therefore, the design of an RLC circuit must consider an operating range below the resonance frequency; for this reason, it is customary to have a resonance at values close to 10 kHz, since approved protocols require pulses with frequencies up to 1 kHz (Fang *et al.*, 2018). For a more in-depth understanding of the resonant frequency, please consult (Ramirez, 2021). The electric circuit provides the power to generate the desired magnetic field. One of the main problems of transcranial magnetic stimulation systems is the heating of the coil, caused by the power dissipation associated with the flow of a high current through this element (about 3 kA). From the electrical point of view, the dissipated power can be reduced by decreasing the current that flows through the inductor. However, the magnitude of the generated magnetic field is determined by the current in the coil; therefore, reducing the current decreases the magnitude of the field.

It is proposed to consider the equivalent inductive value of two or more branches of inductors in parallel to reduce the intensity of current that flows through each unit. However, the consumption of the entire block is the same as that of a single element.

Simulation of the magnetic fields of the TMS system

This section focuses on the 3D analysis of the coil geometries, using the FEM AC/DC module of the Comsol Multiphysics software. Comsol Multiphysics is a simulation environment that uses the finite element method to solve physics-related problems. In this case, the problem domain (system geometry) is the electromagnetic field in the frequency domain described by Maxwell's equations. Here, we consider a homogeneous multiturn model of two coil geometries: single solenoid coil, shown in Figure 4, and Figure-8 coil, shown in Figure 5. The coils are excited with the output parameters of the electrical circuit designed previously. The base geometry consists of 8 concentric coplanar copper wire turns, with an external diameter of 90 mm. The point of interest is the spatial distribution of the magnetic flux densi-

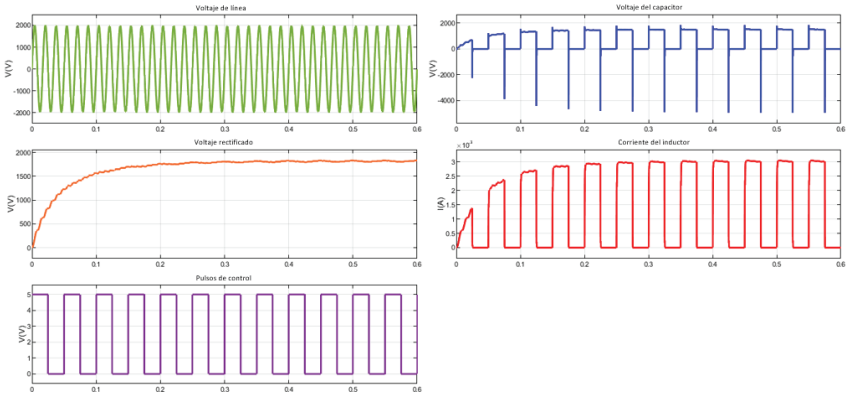

Figure 3. Signals of interest obtained by simulation using Matlab Simulink®

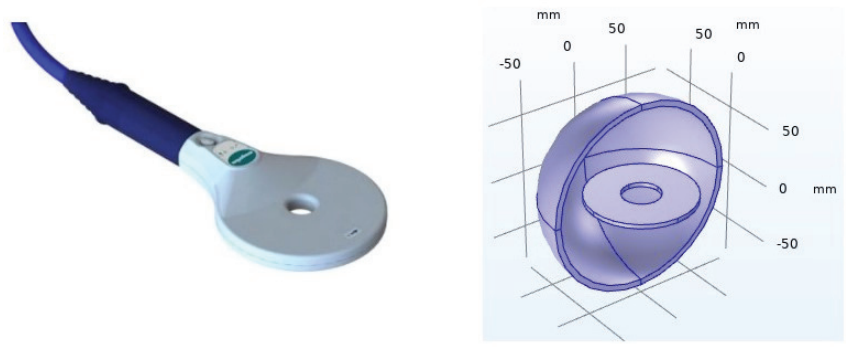

Figure 4. Simple solenoid coil: a) Photo of an actual device [10], b) 3D Model

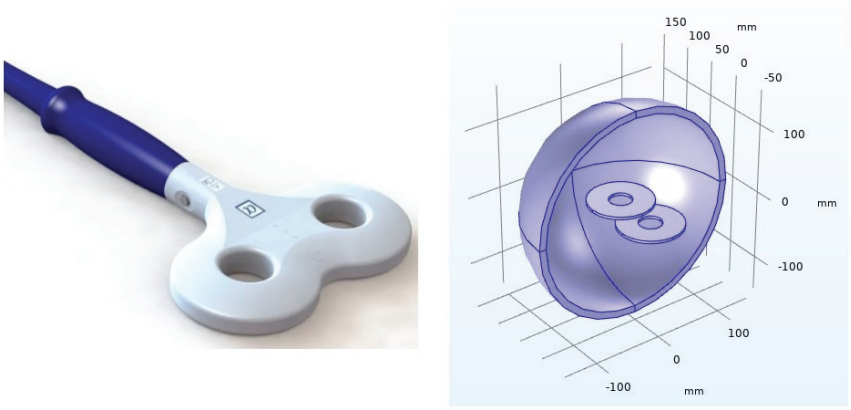

Figure 5. Figure-8 coil: a) Photo of an actual device [10], b) 3D Model

ty B. To do this, a sphere-shaped air domain is added that physically surrounds the coil, considering that this sphere has the boundary condition of a magnetic insulator.

The differential equation governing the magnetic field is derived as follows, in terms of the magnetic vector potential. First, obtaining an expression for the magnetic field intensity H in terms of the magnetic vector potential $\boldsymbol{A}$ (Ramirez, 2021):

$$\boldsymbol{H} = \frac{1}{\mu}\nabla \times \boldsymbol{A} \tag{1}$$

Where μ is the magnetic permeability. The differential equation that fully describes the physics of magnetic fields as a function of a single field variable is (Ramirez, 2021):

$$\nabla \times \left(\frac{1}{\mu}\nabla \times \boldsymbol{A}\right) + \left(j\omega\sigma + \omega^2 \in\right)\boldsymbol{A} - \boldsymbol{J} = 0 \tag{2}$$

Where:

ω = angular frequency with which the magnetic field oscillates

σ and $\in$ = electrical conductivity and electric permittivity of the medium respectively

$\mathbf{J}$ = imposed current density

Equation (2) is a reduced potential formulation for time-harmonic quasi-static systems in terms of the magnetic vector potential. The manuscript exclusively employs the International System of Units (SI) for all quantities.

Additional mathematical expressions related to the finite element method can be consulted in (Ramirez, 2021).

Models for the proposed modified coils were developed to decrease the temperature. These models use concentric coils and are shown in Figure 6 for the simple solenoid geometry and Figure 7 for the Figure-8 geometry model. With these models, a magnetic flux density of the same magnitude as the homogeneous multi-turn model is obtained (Liu *et al.*, 2020), dividing the magnitude of the current intensity by the number of conductors in parallel on different paths. This principle is the basis for reducing the power dissipated in the

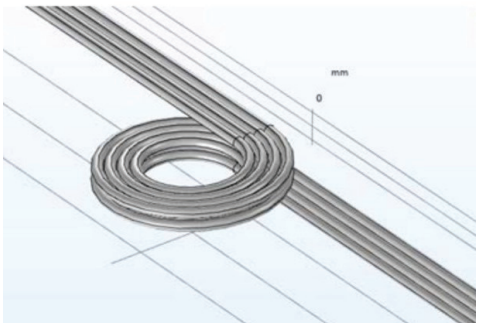

Figure 6. Simple solenoid coil geometry model using concentric conductors

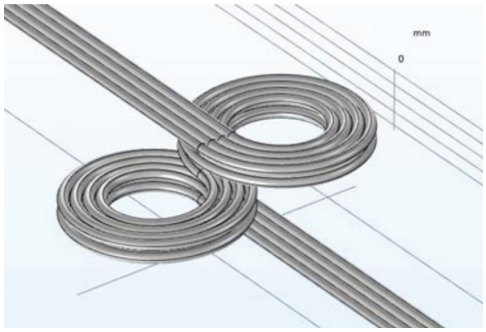

Figure 7. Figure-8-Coil geometry model using concentric conductors

https://doi.org/10.22201/fi.25940732e.2024.25.2.015

form of heat. In addition, the excitation for these models is under the same conditions as with the homogeneous multi-turn model.

We carried out a multiphysics simulation in which the frequency-dependent magnetic field and the currents that generate it serve as sources of heating due to resistive losses. The governing equations of the heat transfer problem are ("COMSOL Multiphysics", n.d.):

$$\rho C_p u \cdot \nabla T + \nabla \cdot q = Q_{rh} + Q_{ml} + Q_{ted} \quad (3)$$

and

$$q = -k\nabla T \quad (4)$$

Here:

ρ = density
Cp = specific heat capacity
u = translational motion velocity vector
T = absolute temperature
q = heat flux
Q_{rh} = resistive losses
Q_{ml} = magnetic losses (in this case they are considered zero since a constant value of magnetic permeability is used)
Q_{tec} = thermoelastic damping in solids
k = thermal conductivity of the material

The expression for the resistive losses is ("COMSOL Multiphysics", n.d.):

$$Q_{rh} = 1/2\ Re\ \{\boldsymbol{J} \cdot \boldsymbol{E}\} \quad (5)$$

Results

Figure 8 shows the curve of the magnetic flux density for the coil with simple conductors (open geometry) on the Z axis, where it can be seen that the magnetic field decays in magnitude to 50 % at a depth of 20 mm. Beyond 70 mm the magnetic field is zero.

Figure 9 shows the spatial distribution of the magnetic flux density generated by the simple solenoid coil model in the XZ plane, within a sphere of 120 mm radius, which delimits the environment within which the flux density is significant. Figure 10 shows the spatial distribution of the magnetic flux density generated by the Figure-8 coil model in the YZ plane.

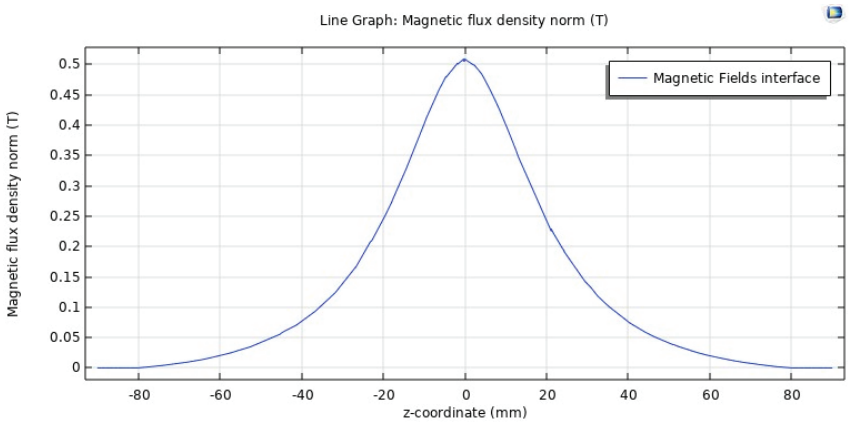

Figure 8. Magnetic flux density on the Z axis for a coil with conductors

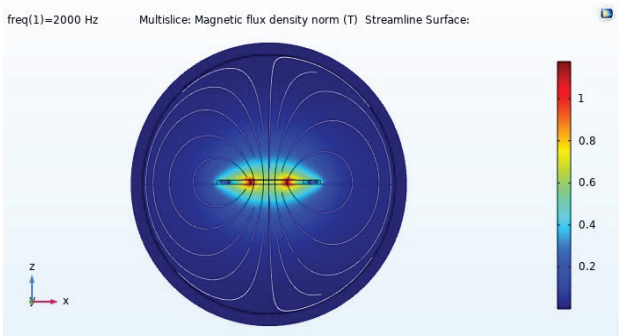

Figure 9. Distribution of magnetic flux density in the surrounding space to the single solenoid coil geometry

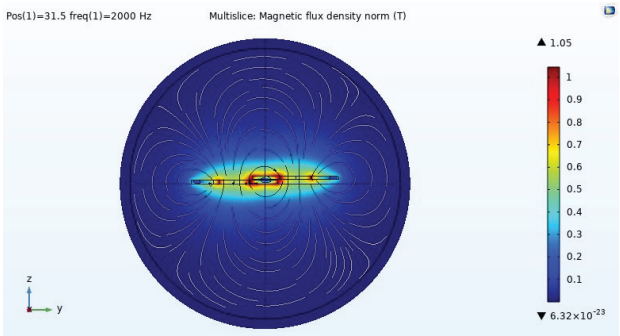

Figure 10. Distribution of magnetic flux density in the surrounding space to the Figure-8 coil geometry

Figure 11 shows the spatial distribution of the temperature reached in the surrounding space in the XZ plane of the simple solenoid stimulation coil after two seconds. This is common in stimulation protocols where pulse trains of up to 2 seconds are used with high internal frequencies, in this case 2 kHz. Figure 12 shows the spatial distribution of the temperature reached in the surrounding space in the YZ plane of the Figure-8 stimulation coil. The maximum operating temperature reached is between 100°C and 120°C.

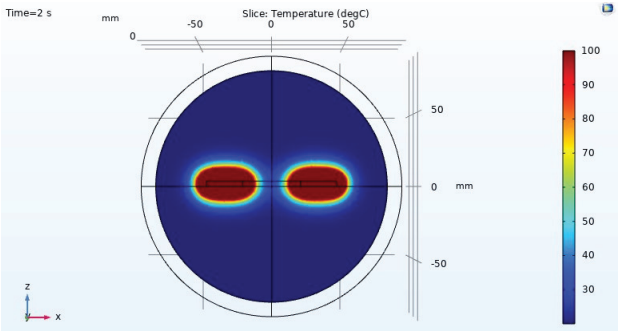

Figure 11. Temperature distribution around the simple solenoid stimulation coil

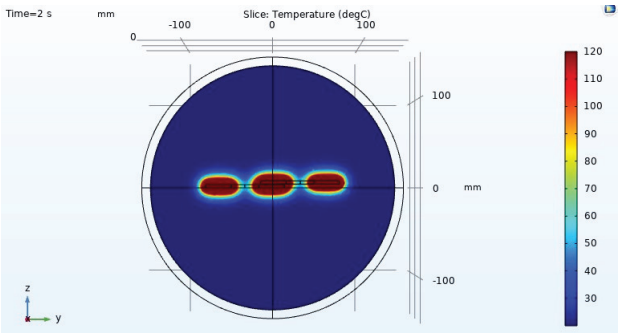

Figure 12. Temperature distribution around the Figure-8 stimulation coil

The thermal response of the proposed coil geometries with concentric conductors is then analyzed. The distribution of the maximum temperature reached by the proposal for the simple solenoid geometry is shown in Figure 13; for the case of the Figure-8 coil geometry, it is shown in Figure 14. In these images, the maximum temperature reached in the surrounding space of both coil geometries is approximately 80°C, which is below the maximum permissible value. This means that less power is dissipated as heat.

From the 22 articles of table A, we obtained some useful comments:

a) Only eight articles manage to reduce the heating of the system coil, although the value of temperature reduction is not mentioned in any. That is why our proposal significantly contributes by reducing the temperature of the coil conductor by 20 °C.
b) In addition to Table A of the literature review, almost 50 % of the publications do not have experimentation due to the complexity of the problem.
c) Also, it is observed that 30 % of the publications do not mention the excitation current of the TMS system.
d) Researchers prefer the finite element method for simulating TMS models, with almost 70 % preference.
e) Finally, most researchers carry out their TMS applications in humans with 80 % and the remaining 20 % in small animals.

Conclusions

A new design for an electric TMS system was proposed, reducing the current of the coils and lowering their operating temperature. We have obtained the following essential results by using a finite element method when

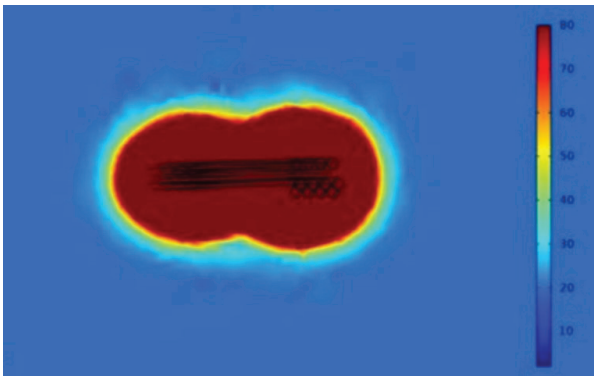

Figure 13. Spatial distribution of temperature around the stimulation coil with simple solenoid geometry using concentric conductors

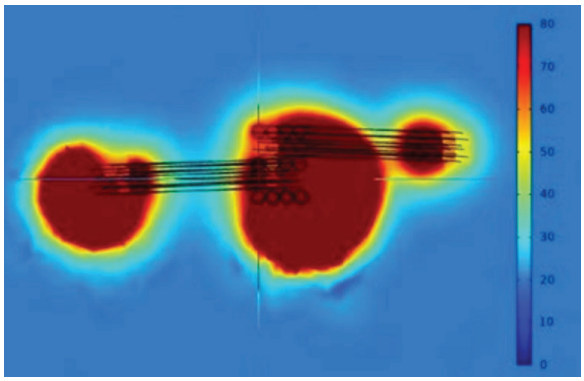

Figure 14. Spatial distribution of temperature around the stimulation coil with Figure-8 geometry using concentric conductors

considering two coil geometries (simple solenoids and Figure-8 geometry):

1. A model with 8 turns of a single conductor is considered, the magnitude of magnetic flux density is consistent with what is reported in commercial equipment domentation. In comparison, if the current is divided into different coils in parallel (4 coils of two turns each), the same magnitude of magnetic flux density is achieved, with less power dissipated.
2. The stimulation coil maximum operating temperature has been lowered by 20°C. This temperature reduction will eliminate the requirement for external cooling systems or their inefficient short-term use, allowing the equipment to be continuously used for longer periods than it can now (currently between 20 and 30 minutes per session).

Then, to take into account the impacts resulting from the simplifications made here, simulations and more extensive modeling will be required before moving further with the manufacturing of this equipment. However, creating more reliable models and complex simulations calls for employing of high-capacity computing hardware. The main limitations of our research are as follows: Given the limitations of the computer hardware at hand, simplified geometric models of the TMS coils (homogeneous multiturn model, homogeneous, and isotropic materials) were employed. Temperature-related changes of the TMS system parameters were not taken into account.

The development of the models presented in this work is a starting point for more detailed coil models with a broad spectrum of applications, such as in vitro models, animal models or clinical tests in patients, where maintaining the operating temperature is crucial for the correct design and application of the stimulation protocol. The repercussions that the development of a magnetic stimulation system entails are important, since this technique has remained stagnant in the clinical aspect, given the equipment's complexity and the high acquisition cost.

The production cost of TMS systems must be decreased as part of future work, considering the materials utilized, manufacturing procedures, useful life, and tests. Simulating the coupling of the excitation circuit with the TMS system coils would be another area to research in the future. It is advised to conduct a magnetic study using a real patient head model while considering the characteristics of the various brain tissues to evaluate the effects of stimulation. As part of future work, we intend to explore alternative pulse trains documented in the existing literature for the switching stage. This exploration will involve utilizing frequencies as listed in Table 1 (Appendix A). It is also relevant to have comparisons with different types of materials.

Appendix A

Table 1. Comparison of other works and the proposed one for TMS systems (continue ...)

Ref	Coil type	Excitation current	Reduce temperature/ power	Experimentation?	Method
(Epstein & Davey, 2002)	Iron-Core coils	-	1,000 pulses over 10 minutes without any interruption due to excess coil temperatures	Yes	Boundary–element analysis
(Salvador *et al.*, 2007)	High-Permeability core coils	-	No	No	Finite elements method
(Ho *et al.*, 2009)	A cone-shaped coil consisting of two circular coils and an array-coil unit which consists of 7 circular coils	A current density of $5X10^8$ A/m flows through the coils	No	No	A genetic algorithm is used to search for the optimal parameters of the coils
(Deng & Peterchev, 2011)	Quadrupole TMS coil configuration that can be electronically switched	-	No	No	Finite element method package MagNet and its 3-D electromagnetic time-harmonic solver
(Talebinejad, *et al.*, 2011)	Coil using rectangular braided litz wire	10 kA, and 3 kV	No	Yes. Four coils were compared	The COMSOL Multiphysics was employed for finite element simulations

Table 1. Comparison of other works and the proposed one for TMS systems (... continue)

Ref	Coil type	Excitation current	Reduce temperature/ power	Experimentation?	Method
(Gomez *et al.*, 2013)	Single-Source Multi-Coil	-	$1/50^{th}$ the current and exciting 3 times less volume than figure-8 TMS coils	No	Pareto genetic algorithm
(Roth *et al.*, 2014)	Multi-channel stimulator, comprising five channels	-	A significant saving in energy consumption and a reduction in coil heating were demonstrated	Yes	The version of the multi-channel "Multiway" stimulator designed included five independent channels
(Yamamoto *et al.*, 2016)	Coil with a laminated iron core plate	The current applied to the coil 3 kA at 3.15 kHz	The current applied to the coil can be considerably reduced by using a combination of laminated iron core plate	No	Finite element method (FEM) simulations
(Rastogi *et al.*, 2016)	Seven mouse TMS coils	5000 A	No	No	SEMCAD X, a finite element analysis tool
(Koponen *et al.*, 2015)	Minimum-energy TMS coils	Typically increased from 0 to over 5000A in less than 100 μs	The optimized coil design requires significantly less power than existing TMS coil designs (a 73 % reduction compared to an existing TMS coil)	Yes	Optimization problem
(Koponen *et al.*, 2017)	Litz wire coils	Peak current below 3000 A	Litz wire coil requires less than half the power of a commercial figure-of-eight coil	Yes	Interior-point-method
(Zhang *et al.*, 2017)	Improved Figure-of-Eight Coil	Various excitation current and operating frequency values are adopted	No	Yes	Finite element method (JMAG)
(Li *et al.*, 2017)	Six figure-of-eight coils of different sizes overlapping with each other at different angles	–	No	Yes	Finite element method
(Selvaraj *et al.*, 2018)	Focused coil for the application of small animals	1000 A at 2.5 Hz	No	Yes	Finite element method
(Fang *et al.*, 2018)	Semiellipse coil pair	The current amplitude is 2600 A at 3 kHz to induce an electrical field of 30 ~ 100 V/m	No	Yes	Finite element method
(Hao *et al.*, 2018)	A multi-circle tangent coil	Sine wave current source with the maximum current of 3000 A at 0.3 Hz	No	No	SEMCAD X, based on finite difference time domain (FDTD) and finite element method (FEM)
(Rastogi *et al.*, 2019)	Deep brain coil-triple halo coil	3500 A (at 70 % of power level) at 2500 Hz	No	Jali Medicals Inc. helped	SEMCAD X and Sim4life (Finite element analysis tools)
(Wei *et al.*, 2019)	Halo coil, HCA coil, HPC coil and HMTC coil	5.0 kA at 2.5 kHz	No	No	Finite element method (ANSYS)
(Liu *et al.*, 2020)	Thin Core Coil	2000 A at 3000 Hz	Compared with other magnetic core coils, the overall coil heat is reduced by 85.1 % ~ 88.8 %	No	Finite element method (COMSOL Multiphysics). MATLAB for optimization

Table 1. Comparison of other works and the proposed one for TMS systems (... continue)

Ref	Coil type	Excitation current	Reduce temperature/ power	Experimentation?	Method
(Zhang *et al.*, 2021)	Quad-form coil	680 A at 13 kHz	No. This is a low intensity application. The calculated maximum magnetic flux density at the target nerve location was 26.1 mT	Yes	Finite element method
(Yu *et al.*, 2022)	Conductive shield and iron core coil	Sinusoidal current of 1 kA (at 2.5 kHz)	No	No	Finite element method (COMSOL Multiphysics)
(Nieminen *et al.*, 2022)	A planar 5-coil transducer	By adjusting the currents in the coils, the induced electric field pattern in the cortex can be modified electronically without coil movement	No	Yes	BEM (Boundary element method)
Proposal	Concentric coils. With this model, the magnitude of the current intensity is divided by the number of conductors in parallel on different paths	3 kA at 2 kHz	The results indicate that the stimulation coil's maximum operating temperature is reduced by 20 °C	**No**	**Finite element method (COMSOL Multiphysics)**

Acknowledgments

The authors would like to thank for the financial support provided by the following Mexican Institutions: CONAHCYT and PRODEP.

References

COMSOL Multiphysics Reference Manual. (N.d.). Retrieved June 1, 2023, from https://doc.comsol.com/5.5/doc/com.comsol.help.comsol/COMSOL_ReferenceManual.pdf

Davey, K., & Epstein, C. M. (2000). Magnetic stimulation coil and circuit design. *IEEE Transactions on Bio-Medical Engineering*, 47(11), 1493-1499. https://doi.org/10.1109/10.880101

Deng, Z.-D., & Peterchev, A. V. (2011). Transcranial magnetic stimulation coil with electronically switchable active and sham modes. Annual International Conference of the IEEE Engineering in Medicine and Biology Society. IEEE Engineering in Medicine and Biology Society. Annual International Conference, 1993-1996. Retrieved on: https://doi.org/10.1109/IEMBS.2011.6090561

Epstein, C. M., & Davey, K. R. (2002). Iron-core coils for transcranial magnetic stimulation. *Journal of Clinical Neurophysiology: Official Publication of the American Electroencephalographic Society*, 19(4), 376-381. https://doi.org/10.1097/00004691-200208000-00010

Epstein, C. M., & Eric, M. (2008). *Oxford Handbook of Transcranial Stimulation*. U. Wassermann, Ed.

Fang, X., Ding, H., Huang, Y., Zhou, J., Wang, Q., & Zhao, Z. (2018). Improved intracranial induced electrical field in transcranial magnetic stimulation with semiellipse coil pair. *IEEE Transactions on Applied Superconductivity: A Publication of the IEEE Superconductivity Committee*, 28(3), 1-6. https://doi.org/10.1109/tasc.2018.2796096

Floyd, T. L. (2019). *Principles of electric circuits: Conventional current version*. Pearson.

Ginou, A., Roth, Y., Levkovitz, Y., Pell, G. S., Ankry, M., & Zangen, A. (2014). Safety and characterization of a novel multi-channel TMS stimulator. *Brain Stimulation*, 7(5), e19. https://doi.org/10.1016/j.brs.2014.07.009

Gomez, L. J., Hernandez-Garcia, L., Grbic, A., & Michielssen, E. (2013). Single-source multi-coil transcranial magnetic stimulators for deep and focused stimulation of the human brain. 2013 USNC-URSI Radio Science Meeting (Joint with AP-S Symposium).

Hao, D., Zhou, Y., Gao, P., Yang, L., Yang, Y., & Chen, F. (2018). Simulation study on coil design for transcranial magnetic stimulation. Annual International Conference of the IEEE Engineering in Medicine and Biology Society. IEEE Engineering in Medicine and Biology Society. Annual International Conference, 2174-2177. Retrieved on: https://doi.org/10.1109/EMBC.2018.8512683

Hardwick, R. M., Lesage, E., & Miall, R. C. (2014). Cerebellar transcranial magnetic stimulation: the role of coil geometry and tissue depth. *Brain Stimulation*, 7(5), 643-649. https://doi.org/10.1016/j.brs.2014.04.009

Ho, S. L., Xu, G., Fu, W. N., Yang, Q., Hou, H., & Yan, W. (2009). Optimization of array magnetic coil design for functional magnetic stimulation based on improved genetic algorithm. *IEEE Transactions on Magnetics*, 45(10), 4849-4852. https://doi.org/10.1109/tmag.2009.2025892

Kaster, T. S., Daskalakis, Z. J., Noda, Y., Knyahnytska, Y., Downar, J., Rajji, T. K., Levkovitz, Y., Zangen, A., Butters, M. A., Mulsant, B. H., & Blumberger, D. M. (2018). Efficacy, tolerability, and cognitive effects of deep transcranial magnetic stimulation for late-life depression: a prospective randomized controlled trial. *Neuropsychopharmacology*, 43(11), 2231-2238. https://doi.org/10.1038/s41386-018-0121-x

Koponen, L. M., Nieminen, J. O., & Ilmoniemi, R. J. (2015). Minimum-energy coils for transcranial magnetic stimulation: application to focal stimulation. *Brain Stimulation*, 8(1), 124-134. https://doi.org/10.1016/j.brs.2014.10.002

Koponen, L. M., Nieminen, J. O., Mutanen, T. P., Stenroos, M., & Ilmoniemi, R. J. (2017). Coil optimisation for transcranial magnetic stimulation in realistic head geometry. *Brain Stimulation*, 10(4), 795-805. https://doi.org/10.1016/j.brs.2017.04.001

Li, Y., Cosoroaba, E., Maharjan, L., & Fahimi, B. (2017). Comparative study of a new coil design with traditional shielded figure-of-eight coil for transcranial magnetic stimulation. *IEEE Transactions on Magnetics*, 54(3), 1-4. https://doi.org/10.1109/tmag.2017.2751260

Liu, C., Ding, H., Fang, X., & Wang, Z. (2020). Optimal design of transcranial magnetic stimulation thin core coil with trade-off between stimulation effect and heat energy. *IEEE Transactions on Applied Superconductivity*, 30(4), 1-6. https://doi.org/10.1109/tasc.2020.2978790

Maertens de Noordhout, A. (2006). General principles for clinical use of repetitive transcranial magnetic stimulation (rTMS). *Neurophysiologie Clinique [Clinical Neurophysiology]*, 36(3), 97-103. https://doi.org/10.1016/j.neucli.2006.08.010

Medicalexpo.com. (N.d.). Retrieved June 1, 2023, from https://www.medicalexpo.com/medical-manufacturer/transcranial-magnetic-stimulator-49038.html

Nieminen, J. O., Sinisalo, H., Souza, V. H., Malmi, M., Yuryev, M., Tervo, A. E., Stenroos, M., Milardovich, D., Korhonen, J. T., Koponen, L. M., & Ilmoniemi, R. J. (2022). Multi-locus transcranial magnetic stimulation system for electronically targeted brain stimulation. *Brain Stimulation*, 15(1), 116-124. https://doi.org/10.1016/j.brs.2021.11.014

Oliviero, A., Mordillo-Mateos, L., Arias, P., Panyavin, I., Foffani, G., & Aguilar, J. (2011). Transcranial static magnetic field stimulation of the human motor cortex: TSMS of the human motor cortex. *The Journal of Physiology*, 589(Pt 20), 4949-4958. https://doi.org/10.1113/jphysiol.2011.211953

Opitz, A., Windhoff, M., Heidemann, R. M., Turner, R., & Thielscher, A. (2011). How the brain tissue shapes the electric field induced by transcranial magnetic stimulation. *NeuroImage*, 58(3), 849-859. https://doi.org/10.1016/j.neuroimage.2011.06.069

Ori, H., Marder, E., & Marom, S. (2018). Cellular function given parametric variation in the Hodgkin and Huxley model of excitability. *Proceedings of the National Academy of Sciences of the United States of America*, 115(35), E8211-E8218. https://doi.org/10.1073/pnas.1808552115

Pastor-Gómez, J. (2000). Fundamentos biofísicos de la actividad neuronal. *Revista de neurología*, 30(08), 741. https://doi.org/10.33588/rn.3008.99539

Ramírez-Galindo, A. (2021). *Computational analysis of electrical circuits and coil geometries for transcranial magnetic stimulation systems.* (Master´s Thesis). Universidad Autónoma Metropolitana, México. Retrieved on https://doi.org/10.1109tmag.2015.2514064

Rastogi, P., Hadimani, R. L., & Jiles, D. C. (2016). Investigation of coil designs for transcranial magnetic stimulation on mice. *IEEE Transactions on Magnetics*, 52(7), 1-4. https://zaloamati.azc.uam.mx/handle/11191/8094

Rastogi-Priyam, L. E. G., Hadimani, R. L., & Jiles, D. C. (2019). Transcranial magnetic stimulation: Development of a novel deep-brain triple-halo coil. *IEEE Magnetics Letters*, 10, 1–5. https://doi.org/10.1109/lmag.2019.2903993

Roth, Y., Padberg, F., & Zangen, A. (2014). Transcranial magnetic stimulation of deep brain regions: Principles and methods. In Transcranial Brain Stimulation for Treatment of Psychiatric Disorders, 204-224. KARGER.

Salvador, R., Miranda, P. C., Roth, Y., & Zangen, A. (2007). High-permeability core coils for transcranial magnetic stimulation of deep brain regions. Annual International Conference of the IEEE Engineering in Medicine and Biology Society. IEEE Engineering in Medicine and Biology Society. Annual International Conference, 6653-6656. Retrieved on https://doi.org/10.1109/IEMBS.2007.4353885

Selvaraj, J., Rastogi, P., Prabhu Gaunkar, N., Hadimani, R. L., & Mina, M. (2018). Transcranial magnetic stimulation: Design of a stimulator and a focused coil for the application of small animals. *IEEE Transactions on Magnetics*, 54(11), 1-5. https://doi.org/10.1109/tmag.2018.2846521

Talebinejad, M., Musallam, S., & Marble, A. E. (2011). A transcranial magnetic stimulation coil using rectangular braided Litz wire. 2011 IEEE International Symposium on Medical Measurements and Applications. Retrieved on https://doi.org/10.1109/MeMeA.2011.5966664

Túnez, I., Drucker-Colín, R., Jimena, I., Medina, F. J., Muñoz, M. del C., Peña, J., & Montilla, P. (2006). Transcranial magnetic stimulation attenuates cell loss and oxidative damage in the striatum induced in the 3-nitropropionic model of Huntington's disease: TMS and Huntington's disease. *Journal of Neurochemistry*, 97(3), 619-630. https://doi.org/10.1111/j.1471-4159.2006.03724.x

Van den Noort, M., Yeo, S., Lim, S., Lee, S.-H., Staudte, H., & Bosch, P. (2018). Acupuncture as add-on treatment of the positive, negative, and cognitive symptoms of patients with schizophrenia: A systematic review. *Medicines* (Basel, Switzerland), 5(2). https://doi.org/10.3390/medicines5020029

Vlachos, A., Müller-Dahlhaus, F., Rosskopp, J., Lenz, M., Ziemann, U., & Deller, T. (2012). Repetitive magnetic stimulation induces functional and structural plasticity of excitatory postsynapses in mouse organotypic hippocampal slice cultures. *The Journal of Neuroscience*, 32(48), 17514-17523. https://doi.org/10.1523/JNEUROSCI.0409-12.2012

Wei, X., Shi, D., Lu, M., Yi, G., & Wang, J. (2019). Deep transcranial magnetic stimulation: Improved coil design and assessment of the induced fields using realistic head model. 2019 Chinese Control Conference (CCC).

Yamamoto, K., Miyawaki, Y., Saitoh, Y., & Sekino, M. (2016). Improvement in efficiency of transcranial magnetic stimulator coil by combination of iron core plates laminated in different directions. *IEEE Transactions on Magnetics*, 52(7), 1-4. https://doi.org/10.1109/tmag.2016.2514321

Yu, H., Du, B., Guo, L., & Xu, G. (2022). Design of transcranial magnetic stimulation coils for mouse with improved stimulus focus and intensity. *IEEE Transactions on Magnetics*, 58(2), 1-4. https://doi.org/10.1109/tmag.2021.3084451

Zanardini, R., Gazzoli, A., Ventriglia, M., Perez, J., Bignotti, S., Rossini, P. M., Gennarelli, M., & Bocchio-Chiavetto, L. (2006). Effect of repetitive transcranial magnetic stimulation on serum brain derived neurotrophic factor in drug resistant depressed patients. *Journal of Affective Disorders*, 91(1), 83-86. https://doi.org/10.1016/j.jad.2005.12.029

Zhang, N., Wang, Z., Shi, J., Ning, S., Zhang, Y., Wang, S., & Qiu, H. (2021). Theoretical analysis and design of an innovative coil structure for transcranial magnetic stimulation. *Applied Sciences* (Basel, Switzerland), 11(4), 1960. https://doi.org/10.3390/app11041960

Zhang, Z., Ai, W., Deng, B., Han, W., & Wang, J. (2017). Improved figure-of-eight coil for transcranial magnetic stimulation using magnetic resonant coupling. *IEEE Transactions on Magnetics*, 53(11), 15. https://doi.org/10.1109/tmag.2017.2700319

Cómo citar:

Ramirez-Galindo, A. D., Olivares-Galvan, J. C., Corona-Sánchez, M. A., Escarela-Perez, R., Melgoza-Vazquez, E., & Gonzalez-Montañez, F. de J. (2024). Efficient coil design for transcranial magnetic stimulation using computational tools. *Ingeniería Investigación y Tecnología*, 25(02), 1-12. https://doi.org/10.22201/fi.25940732e.2024.25.2.015